

Article

Spatial Mapping of Air Pollution Hotspots around Commercial Meat-Cooking Restaurants Using Bicycle-Based Mobile Monitoring

Gwang-Soon Yong¹, Gun-Woo Mun¹ and Kyung-Hwan Kwak^{2,3,*} 

¹ School of Natural Resources and Environmental Science, Kangwon National University, Chuncheon 24341, Republic of Korea; yong_5286@naver.com (G.-S.Y.); gunwoo9502@naver.com (G.-W.M.)

² Department of Environmental Science, Kangwon National University, Chuncheon 24341, Republic of Korea

³ Gangwon Particle Pollution Research and Management Center, Kangwon National University, Chuncheon 24341, Republic of Korea

* Correspondence: khkwak@kangwon.ac.kr

Abstract: Mobile measurement techniques are increasingly utilized to monitor urban emissions, regional air quality, and air pollutant exposure assessments. This study employed a bicycle measurement method to obtain the detailed distribution of air pollutant concentrations in roadside, commercial, residential, and recreational areas. The study area is located in Chuncheon, South Korea, with approximately 280,000 residents. Black carbon (BC), PM_{2.5}, and NO₂ were monitored using portable devices equipped on an electric bicycle. Results showed that in the evening (6–8 p.m.), the concentrations were higher in both commercial and residential areas compared to the background location, while concentrations were notably elevated only in roadside areas in the morning (8–10 a.m.). Spatial mapping of measured concentrations revealed that the highest concentrations corresponded to areas with densely operated charbroiling meat-cooking restaurants. Additionally, it was confirmed that BC and PM_{2.5} emitted from the commercial areas influenced nearby recreational areas (e.g., streamside roads). In conclusion, this study demonstrated that air pollutant hotspots resulting from human activities, such as dining at commercial restaurants, significantly worsen the local air quality on a small scale. Efforts to reduce the uncontrolled emissions of air pollutants from charbroiling meat-cooking restaurants are necessary.

Keywords: air pollution hotspots; commercial meat-cooking restaurants; mobile monitoring; particulate matter (PM); black carbon (BC)



Citation: Yong, G.-S.; Mun, G.-W.; Kwak, K.-H. Spatial Mapping of Air Pollution Hotspots around Commercial Meat-Cooking Restaurants Using Bicycle-Based Mobile Monitoring. *Atmosphere* **2024**, *15*, 991. <https://doi.org/10.3390/atmos15080991>

Academic Editors: Zhaobin Sun, Jun Yang and Ling Han

Received: 10 June 2024

Revised: 8 August 2024

Accepted: 14 August 2024

Published: 17 August 2024



Copyright: © 2024 by the authors. Licensee MDPI, Basel, Switzerland. This article is an open access article distributed under the terms and conditions of the Creative Commons Attribution (CC BY) license (<https://creativecommons.org/licenses/by/4.0/>).

1. Introduction

Air pollutant emission sources in urban areas are mainly classified into the energy, industry, transportation, and living sectors. One of the major emission sources in the living sector is biomass burning due to cooking and heating. According to the national air pollutant emissions of 2021 [1], the PM_{2.5} (i.e., particulate matter with an aerodynamic diameter of less than 2.5 μm) emission amount from biomass burning accounted for 20.1% in 2021 in South Korea, which is the third largest emission category after fugitive dust (28.8%) and non-road transport (25.9%). The PM and other air pollutants emitted from cooking and heating sources are known to be closely related to human health due to the proximity of residential areas to their emission sources in the urban micro-environment [2]. While the emission inventories in the energy, industry, and transport sectors have been systematically estimated based on nationwide annual statistical data, the reliability of emission inventories of biomass burning in the living sector remains uncertain due to deficient onsite activity data and undeveloped emission factors [3]. Therefore, the lack of reliable emission data from biomass-burning sources makes it difficult for government officers to regulate air pollutant emission sources.

The amount of PM_{2.5} emitted by cooking depends on food ingredients, cooking methods and utensils, fuels, etc. [4] Among a number of other restaurants, commercial meat-cooking restaurants have been regarded as the dominant PM_{2.5} emission sources in urban residential and commercial areas. The PM_{2.5} emission factor of raw meat grilling is estimated to be the largest for chicken, followed by pork, beef, and duck [5]. In addition, the PM_{2.5} emission factor from charbroiling, one of the most widely used meat grilling methods, is more than four times larger than that from pan grilling [5]. The large portions of emitted PM_{2.5} by meat cooking consist of organic and element carbon, as well as oil mist [6,7]. Jeong and Park (2017) [8] reported that the black carbon (BC) inhalation rate was elevated up to 0.48 m³ h⁻¹ for an age group of 6–10 years and 0.50 m³ h⁻¹ for an age group of 11–18 years during cooking activity in South Korea. On the other hand, activity patterns of air pollutant emission sources by meat cooking are difficult to standardize statistically in terms of the time of day, day of the week, seasonality, and floating population [9]. Therefore, the air pollution levels and the resultant human exposure to harmful air pollutants need to be estimated based on onsite information on air pollutant emission sources, such as meat-cooking restaurants.

To assess the neighborhood-scale air quality in urban areas, mobile monitoring vehicles equipped with air pollutant analyzers have been widely used in cities worldwide, for example, in Los Angeles, USA [10]; Durham, USA [11]; Hong Kong, China [12]; Seoul, South Korea [13]; Antwerp, Belgium [14]; and Nanjing, China [15]. Full-scale mobile laboratories utilizing customized vans and trucks are beneficial to provide comprehensive air quality information acquired at a selected air pollution hotspot or while driving along a selected route for up to a few hours. Kim et al. [16] built a 2D gridded air pollution map with a high resolution of 50 m × 50 m in a densely populated urban area of Seoul, South Korea, based on mobile measurement using a fully equipped air pollution monitoring van. In the study, although a zone-averaged air pollution level was categorized as the ‘Moderate’ category, at least the top 25% of cell-based air pollution levels, especially near roadways and commercial areas, were likely to be categorized into the ‘Unhealthy’ category or even higher one.

In comparison to the mobile measurements using full-scale vans/trucks mainly investigating traffic-related air pollutants, some recent studies have utilized a bicycle equipped with portable measurement devices and low-cost sensors to assess the neighborhood-scale air quality in urban residential areas behind main roadways. The advantages of mobile measurements using a bicycle are zero self-emissions of the vehicle, accessibility to non-road areas, and visualization at a high spatial resolution with a low driving speed and high temporal resolution. In addition to the strong impacts of vehicle exhaust emissions on neighborhood-scale air quality [17–20], air pollutants emitted from domestic wood-burning sources [21] and construction sites [22,23] have also been successfully detected using bicycle-based mobile platforms. Thus, mobile monitoring using a bicycle enables us to identify air pollution hotspots around different emission sources in a neighborhood-scale urban area.

The aim of this study is to perform the spatial mapping of air pollution around biomass-burning emission sources in urban residential and commercial areas. As many small-sized grill restaurants are excluded from the air pollutant national emission inventories, the air pollution emission amounts from biomass burning by cooking are still largely underestimated [24]. Chuncheon is famous for charbroiling chicken nationwide. Although there are few massive air pollutant emission sources, such as national industrial complexes and coal-fired power plants, in the urban area, urban air quality in Chuncheon is known to be worse than that in metropolitan cities of South Korea [25,26]. In this study, we develop a bicycle-based mobile platform and perform mobile monitoring along the selected route around commercial meat-cooking restaurants in Chuncheon, South Korea. The monitoring results are visualized at a high resolution to analyze air pollution hotspots.

2. Methods

2.1. Study Site and Period

The site of interest is a commercial area located near a railway station in Chuncheon, Gangwon province, Republic of Korea (37.86° N, 127.72° E). Chuncheon, the capital city of Gangwon province, with approximately 280,000 residents, serves as a gateway of Gangwon province to the Seoul metropolitan area and vice versa. There are 85 restaurants and cafeterias in total densely operated in the commercial area of 0.12 km^2 (Figure 1). Out of the 85 restaurants and cafeterias, 29 are charbroiling restaurants of beef, pork, chicken, and duck, opening from noon to late evening (approximately 10 p.m.). Notably, only 4 non-charbroiling restaurants are open in the morning among them. A roadside air quality monitoring station (RAQMS) placed at the corner of the road intersection southwest of the commercial area continuously measures the hourly averaged concentrations of air pollutants, such as PM_{10} , $\text{PM}_{2.5}$, and nitrogen dioxides (NO_2). A stream, called Gongjicheon, flowing through the inner city next to the commercial area is a vital place for citizens' recreational activities. Therefore, we selected a location in the middle of the pedestrian bridge crossing the stream as the background (BG) location.



Figure 1. Mobile monitoring routes passing through roadside, commercial, residential, and stream areas in Chuncheon, Gangwon province, Republic of Korea. The map at the left bottom corner shows the entire Chuncheon basin. The roadside air quality monitoring station (RAQMS) and background (BG) location are indicated by red squares.

The period for mobile monitoring was on selected weekdays from 28 January to 5 March 2021 because local air quality frequently becomes severe during this cold season. The mobile monitoring was conducted in the morning (8–10 a.m.) on five days and evening (6–8 p.m.) on six days non-consecutively, for the purpose of identifying local air pollution hotspots attributed to commuting and dining activities. We avoided the days with high background concentrations of air pollutants (i.e., $\text{PM}_{2.5} \geq 40\ \mu\text{g m}^{-3}$) because the measured concentrations could be influenced by changing the background concentration during a single run when the background concentration is high and fluctuating. We also avoided the days with severe weather conditions, such as heavy precipitation, cold waves, and wind gusts. The monitoring days were 28th (p.m.) and 29th (a.m., p.m.) January, 5th (a.m.), 24th (a.m., p.m.), and 25th (a.m., p.m.) February, and 4th (p.m.) and 5th (a.m., p.m.) March. The daily minimum temperatures were always below $0\ ^{\circ}\text{C}$ and no precipitation occurred on the monitoring days. While the morning-hour monitoring aims to conduct the spatial mapping of air pollutants mainly emitted from on-road traffic emission sources, the evening-hour monitoring aims to detect those mainly emitted from meat-cooking restaurants as well as from on-road traffic emission sources.

2.2. Mobile Monitoring by Bicycle

An electric bicycle with a throttle and speed monitor was used as the bicycle-based mobile monitoring platform (Figure 2). It is highly advantageous for mobile monitoring because a rider can monitor the speed of the bicycle and keep it constant, regardless of road environment such as surface type and slope. As shown in Figure 1, the 7 km-long monitoring route started at the RAQMS and returned to the starting point through the roadside sidewalk, commercial area A, commercial area B, residential area, and Gongjicheon stream. Every run took approximately 45–50 min, with a speed of less than 11 km/h. Two runs in the morning (8–10 a.m.) and two runs in the evening (6–8 p.m.) were repeatedly carried out for the selected days.

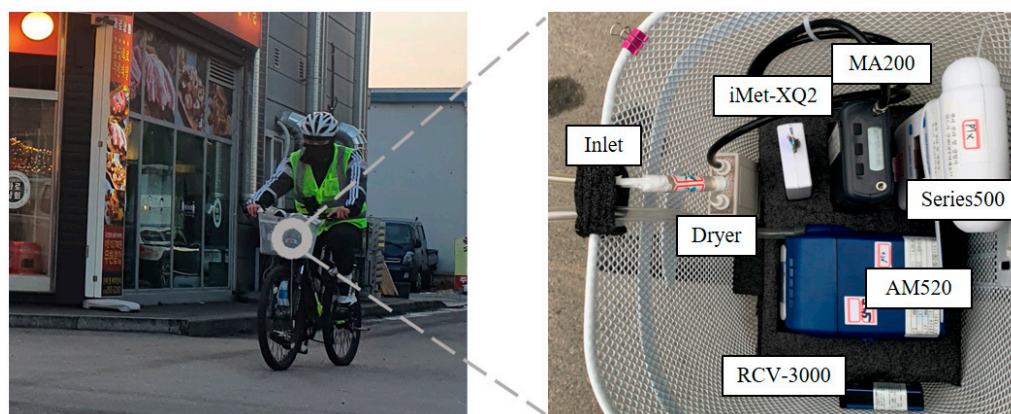


Figure 2. An electric bicycle-based mobile monitoring platform (left) and the deployment of portable devices for measuring particulate and gaseous pollutants in the front basket (right).

Meteorological (Imet-XQ2, InterMet Inc., Grand Rapids, MI, USA, for air temperature and relative humidity), particulate (Sidepak AM520, TSI Inc., Shoreview, MN, USA, for $PM_{2.5}$ and MA200, AethLabs, San Francisco, CA, USA, for BC), and gaseous (Series500, Aeroqual, Auckland, New Zealand, for NO_2) pollutant sensors were deployed in the front basket of the electric bicycle (Table 1). Reliable performances both for air temperature and relative humidity were obtained while testing the meteorological sensor (Imet-XQ2) with a reference sensor in a calibration chamber [27]. The comparison results of particulate pollutant sensors (Sidepak AM520 and MA200) with reference sensors were obtained in roadside environments, showing the coefficient of determination higher than 0.94 and 0.87, respectively [28,29]. A GPS logger (RCV-3000, AscenKorea, Seoul, Republic of Korea) was also equipped to record locational information (e.g., latitude and longitude). The micro-aethalometer for BC measurement was connected to a diffusion dryer prior to its inlet to keep the measurement away from humidity interference [30]. The inlets of particulate pollutants were tied to the front edge of the basket as closely as possible in order to minimize particle losses on inlet tubes.

Table 1. Specifications of instruments used for mobile monitoring.

Variable	Model	Resolution	Flow Rate ($L\ min^{-1}$)	Time Interval (s)
Air temperature/Relative humidity	Imet-XQ2	0.01 °C, 0.1%	-	1
BC	MA200	0.001 $\mu g\ m^{-3}$	0.15	5
$PM_{2.5}$	AM520	1 $\mu g\ m^{-3}$	1.7	1
NO_2	Series500	0.001 ppm	-	60
Location	RCV-3000	-	-	1

2.3. Data Processing

Portable devices used for mobile monitoring do not guarantee the reliability of measured concentrations without a bias correction because the data are frequently influenced by many environmental factors [31]. We recorded the PM_{2.5} and NO₂ concentrations at the start location next to the RAQMS for every run and compared the measured concentrations with those from the RAQMS (Figure 3). The portable devices generally have reasonable sensitivity (enough to detect air pollution hotspots). The PM_{2.5} and NO₂ concentrations measured immediately with time intervals of 1 s and 1 min, respectively, using portable devices commonly, showed small slopes (0.560 and 0.444, respectively) against those at the RAQMS. After correcting such biases of mobile monitoring by applying the regression equations to the measured concentrations, the corrected PM_{2.5} and NO₂ concentrations were used for analysis, similar to a previous study [32].

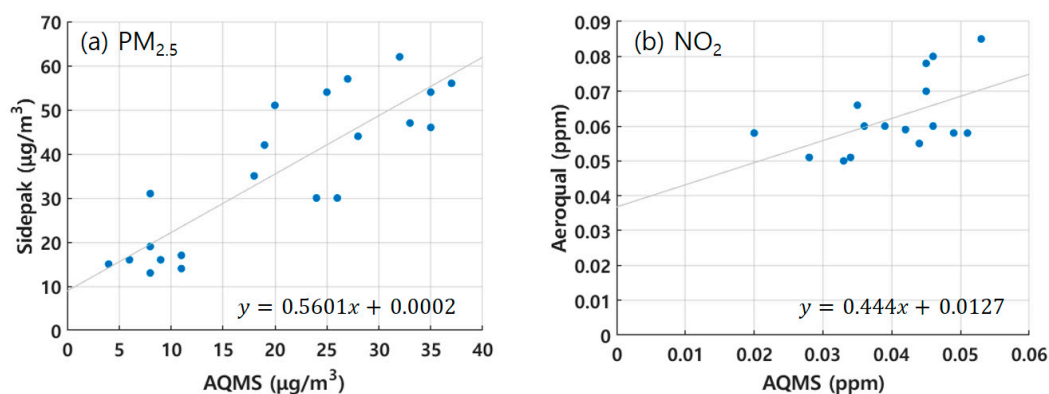


Figure 3. Comparisons of (a) PM_{2.5} and (b) NO₂ concentrations between portable devices (Sidepak and Aeroqual, respectively) and the RAQMS. The inserted equations used for bias correction were obtained via linear regressions between them.

The temporal concentration data recorded at a constant time interval were converted to spatial concentration data at a constant grid cell size in three steps [33,34]. First, the measured concentration data were allocated into grid cells with a 30 m × 30 m size for each run. For example, a cycling speed of 11 km/h (i.e., ~3 m/s) corresponds to more than 10 measurement points in a grid cell with a 30 m × 30 m size for each run, which means that cycling at the lower speed or stopping would allocate the larger number of data in the grid cell. Second, a representative concentration at a grid cell for each run was calculated as a median concentration of allocated data for the grid cell. Finally, the representative concentration at the grid cell is the median of representative concentrations at the grid cell for entire runs when the number of valid representative concentration data is larger than 2 out of 10 (in the morning) and out of 11 (in the evening). This process improves the reliability of spatial mapping data by assuring their independence from the inconstant speed of the bicycle and the uncertainty of GPS logging data.

3. Results and Discussion

To capture air pollution hotspots in the commercial areas, the measured BC and PM_{2.5} concentrations were spatially mapped according to the simultaneously recorded location data (Figure 4). In the morning, the BC concentrations were high along the roadside route, especially near the railway station. On-road BC emission from traffic sources was obviously the major contributor to the elevated BC concentration in the morning, as previously reported in Chuncheon [35,36]. On the other hand, the PM_{2.5} concentrations were lower than 40 µg m⁻³ and showed a smaller spatial variation compared to BC concentrations. While PM_{2.5} comprises BC and other primary and secondary components, the BC portion in PM_{2.5} was approximately 2–10% in the morning during the mobile monitoring period.

Thus, the local traffic emission was found to be less influential to the spatial variability of the $PM_{2.5}$ concentration than background influences such as long-range transport [31].

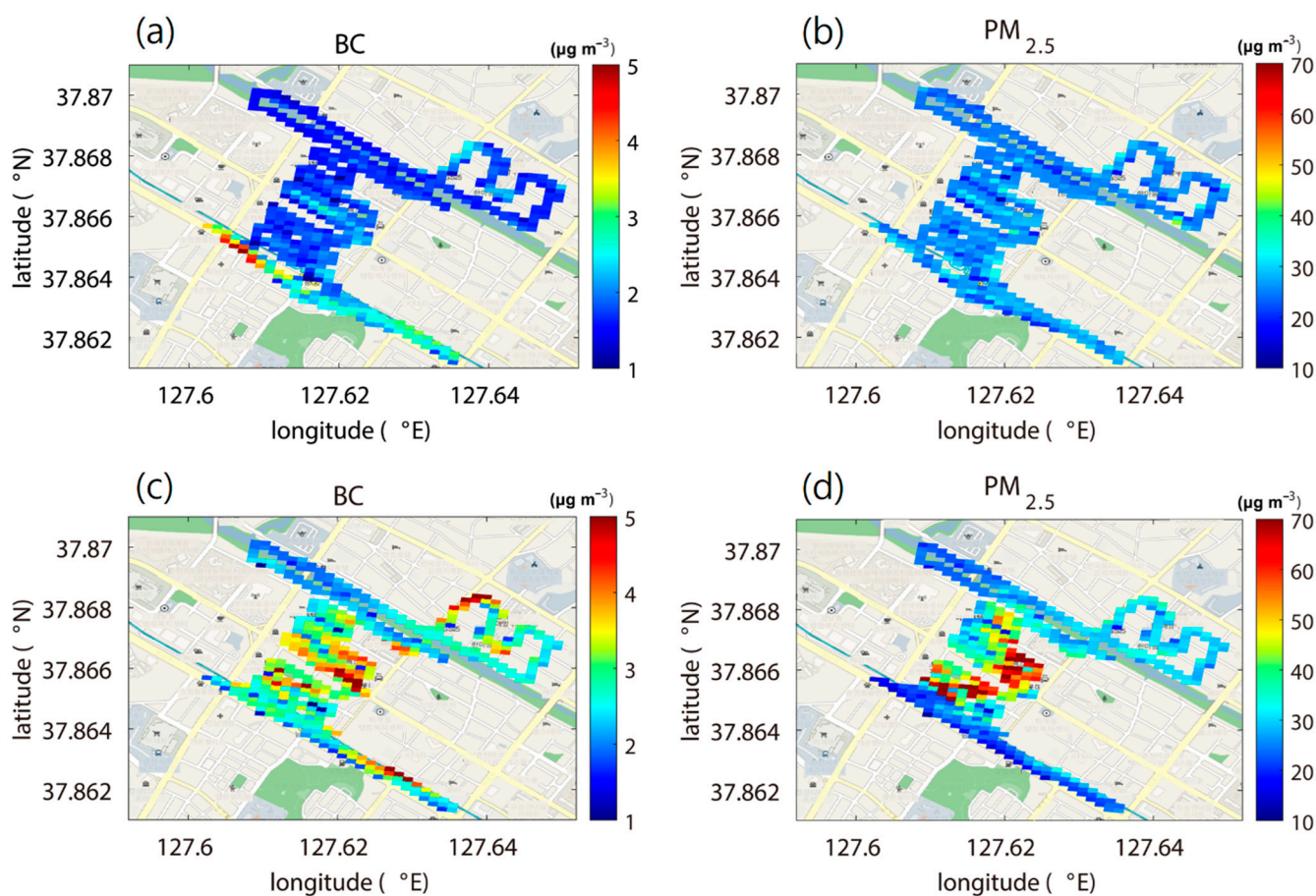


Figure 4. Spatial distributions of (a,c) BC and (b,d) $PM_{2.5}$ concentrations along the mobile monitoring route in the (a,b) morning (8–10 a.m.) and (c,d) evening (6–8 p.m.).

In the evening, hotspots in BC concentrations differed from those in the morning. The BC concentration in the evening, compared to that in the morning, was higher and showed a larger spatial variation. The highest BC concentration appeared at approximately $5 \mu\text{g m}^{-3}$ in commercial area B, with 52 restaurants, including 15 charbroiling ones, mostly opening in the evening. It is noteworthy that none of the charbroiling restaurants was open in the morning. The $PM_{2.5}$ concentration showed a large spatial variation in the evening, which also differed from that in the morning. A couple of hotspots with $PM_{2.5}$ concentrations higher than $60 \mu\text{g m}^{-3}$ were consistent with the hotspots with BC concentrations in commercial area B. The $PM_{2.5}$ concentration was also high in commercial area A, with 33 restaurants, including 14 charbroiling ones, mostly opening in the evening. In contrast to the hotspots found in commercial areas A and B, the BC and $PM_{2.5}$ concentrations were relatively low in the residential area and Gongji-cheon stream. The large discrepancy in the concentrations between analyzed areas implies the large contribution of local BC and $PM_{2.5}$ emissions to the aforementioned air pollution hotspots, particularly in the evening.

We compared the measured BC, $PM_{2.5}$, and NO_2 concentrations on the roadside sidewalk, in commercial areas A and B, in the residential area, and in the Gongji-cheon stream quantitatively (Figure 5). Here, the Gongji-cheon stream route is subdivided into stream A (northside) and B (southside) routes. The roadside sidewalk route obviously showed high BC and NO_2 concentrations in the morning. The increments in concentrations were attributed to the adjacent on-road traffic emission during the morning rush hour. Commercial area B showed the highest median BC and $PM_{2.5}$ concentrations (3.2 and

34.4 $\mu\text{g m}^{-3}$, respectively) in the evening among the categorized routes. In commercial area B, the median BC and $\text{PM}_{2.5}$ concentrations in the evening were 60% and 27%, respectively, higher than those in the morning. Similarly, in commercial area A, the median BC and $\text{PM}_{2.5}$ concentrations (2.9 and 31.0 $\mu\text{g m}^{-3}$, respectively) in the evening were 45% and 14%, respectively, higher than those in the morning. The differences in median BC, $\text{PM}_{2.5}$, and NO_2 concentrations between commercial areas A and B were negligible in the morning when none of the charbroiling restaurants were open. As a result, the increases in concentrations in the evening, especially in commercial area B, were found to be mainly attributed to local emissions from operating charbroiling and other restaurants [37,38]. It is also interesting that many outliers of BC (up to $\sim 16 \mu\text{g m}^{-3}$) and $\text{PM}_{2.5}$ (up to $\sim 200 \mu\text{g m}^{-3}$) concentrations were frequently measured in commercial areas during the mobile monitoring in the evening. We experienced that the outliers were detected on device monitors when the bicycle passed beside the small-sized charbroiling restaurants with directly emitted fumes possibly without operating control or filtration system [39].

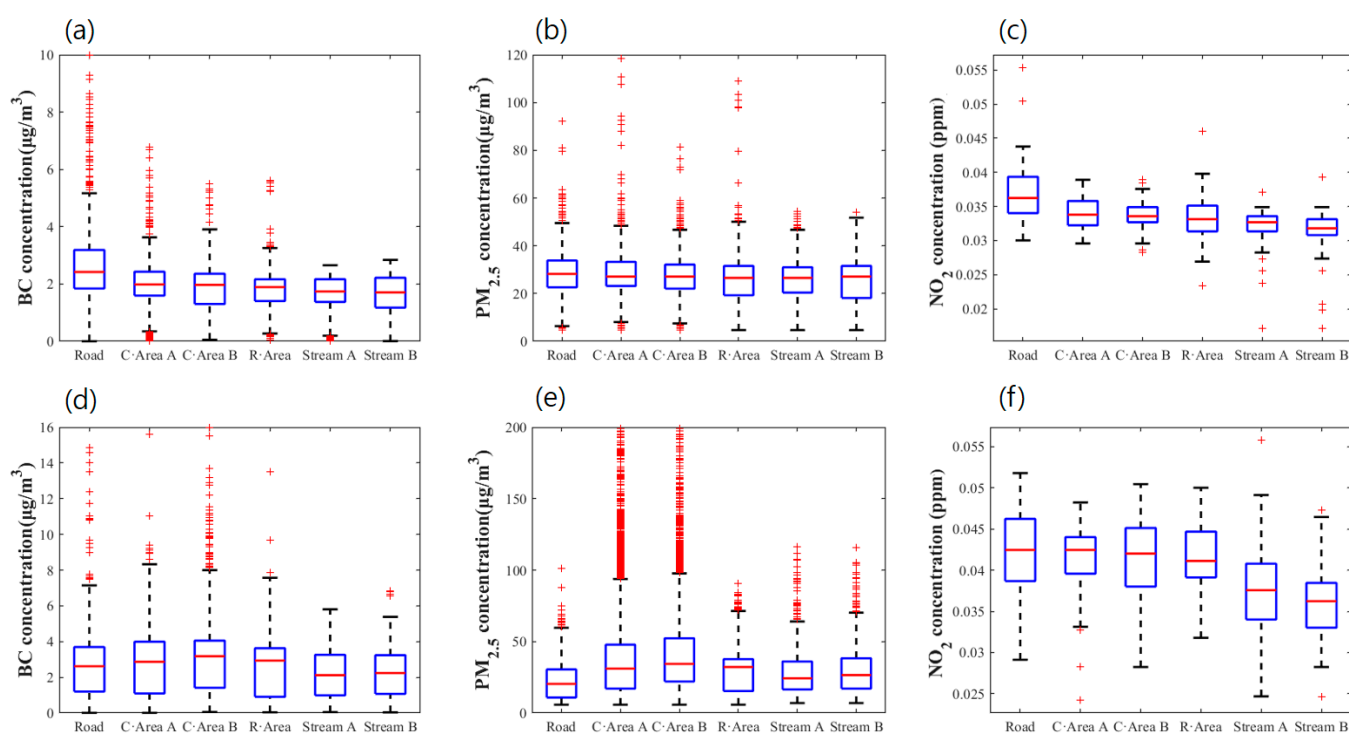


Figure 5. Boxplots of (a,d) BC, (b,e) $\text{PM}_{2.5}$, and (c,f) NO_2 concentrations on the roadside sidewalk (Road), in commercial areas A (C·Area A) and B (C·Area B), in the residential area (R·Area), and in Gongji-cheon streams A (Stream A) and B (Stream B) in the (a–c) morning (8–10 a.m.) and (d–f) evening (6–8 p.m.). Red crosses indicate the outliers of concentration, where blue boxes indicate the range of concentration between first to third quartiles.

We calculated the increase in the ratios of BC, $\text{PM}_{2.5}$, and NO_2 concentrations on the roadside sidewalk, in commercial areas A and B, in the residential area, and in Gongji-cheon streams A and B against their background concentrations measured at the BG location on a bridge over Gongji-cheon stream (Table 2). As shown in Figure 4, the spatial variabilities of BC, $\text{PM}_{2.5}$, and NO_2 concentrations were larger in the evening than in the morning. In the evening, the increases in BC and $\text{PM}_{2.5}$ concentrations were the largest in commercial area B (88% and 64%, respectively), followed by residential area (76% and 54%, respectively) and commercial area A (72% and 48%, respectively). The increase in NO_2 concentration in the commercial area was comparable to that on the roadside in the evening, while the increase in NO_2 concentration was not as large as that on the roadside in the morning. This is probably due to the impact of vehicles driven by restaurant visitors in commercial

areas. In contrast, the increases in concentrations were the smallest in stream A for BC, the roadside sidewalk for PM_{2.5}, and stream B for NO₂. It is noteworthy that the increases in BC and PM_{2.5} concentrations were larger in stream B than in stream A because the distance to commercial area A is shorter from stream B than from stream A. Considering that there is no local BC and PM_{2.5} emission source in the Gongji-cheon stream routes, the higher increase in ratios in stream B than in stream A was obviously influenced by nearby BC and PM_{2.5} emissions from the densely located meat-cooking restaurants in commercial area B. In stream A, the increase in ratios of BC and PM_{2.5} concentrations (26% and 17%, respectively) was still not negligible in the evening, implying the considerable influences from the meat-cooking restaurants in commercial area B to downwind residential and recreational areas within a hundred meter [40]. Notably, the concentration maps show the plumes dispersed from commercial areas to Gongji-cheon stream A and B areas. As a result, the locally emitted BC and PM_{2.5} from meat-cooking restaurants, especially charbroiling restaurants, were found to contribute to elevating their concentrations severely in the neighboring areas, including citizens' recreational places, located within a hundred meters.

Table 2. The increase in ratios of BC, PM_{2.5}, and NO₂ concentrations against their background concentrations.

Area	BC (%)		PM _{2.5} (%)		NO ₂ (%)	
	Morning	Evening	Morning	Evening	Morning	Evening
Roadside	57	57	4	−2	9	23
Commercial A	28	72	0	48	3	23
Commercial B	26	88	0	64	3	23
Residential	23	76	−1	54	0	20
Stream A *	12	26	−1	17	0	11
Stream B **	10	34	0	27	−3	6

* The shortest distance from commercial area B to stream A is 75 m. ** The shortest distance from commercial area B to stream B is 35 m.

We further discuss the remaining influential factors on air pollutant concentrations and distributions during the mobile monitoring days. At first, one of the major socio-economic factors is the impact of social distancing to prevent the spread of the COVID-19 pandemic. During the monitoring period, private gatherings of five or more people were not allowed in indoor restaurants. Because of the social distancing measure, the air pollutant emission amounts in the years 2020 and 2021 were obviously decreased compared to those in the year 2019 [41], which also potentially decreased the contribution of BC and PM_{2.5} emissions in the monitoring areas. This was also one of the influencing factors for the large increase in BC and PM_{2.5} concentrations in residential areas in the evening. Another influential factor is biomass burning activities in suburban areas especially for cold-surge events [42]. There were a couple of days experiencing cold surges with a daily minimum air temperature below −10 °C. Although we excluded monitoring data for the days with strong cold surges from the data analysis, the influence of biomass burning in suburban areas on air pollutant concentrations might be non-negligible.

4. Conclusions

In this study, we selected 11 cases in the morning and evening from 28 January to 5 March 2021 and conducted mobile monitoring of BC, PM_{2.5}, and NO₂ concentrations by riding an electric bicycle on the roadside, commercial area, residential area, and streamside in Chuncheon, South Korea. In the morning, BC, PM_{2.5}, and NO₂ concentrations were highest on the roadside, indicating that traffic emissions had a significant impact on the air pollutant concentrations. On the other hand, BC, PM_{2.5}, and NO₂ concentrations in the evening all showed a couple of hotspots in commercial areas compared to those in the morning, and BC and PM_{2.5} showed higher concentrations in commercial areas than in the roadside area. In particular, their peak concentrations were found near charbroiling meat-cooking restaurants.

We understand that there are some limitations on controlling other influential factors to BC, PM_{2.5}, and NO₂ concentrations. The measurement devices used in this study are portable and equipped on a moving bicycle, which can make some biases that have to be corrected by regression equations. The mobile monitoring was conducted during a period when human activities were reduced due to social distancing where private gatherings of five or more people were prohibited to prevent the spread of the COVID-19 pandemic.

Despite the above limitations, the mobile monitoring conducted in this study confirmed that the impact of BC and PM_{2.5} emission sources in daily life is non-negligible and the results of this study show that efforts to reduce the air pollutants, particularly particulate pollutants, emitted from charbroiling meat-cooking restaurants in the evening are necessary.

Author Contributions: Conceptualization, K.-H.K.; formal analysis, G.-S.Y.; validation, G.-S.Y.; investigation, G.-S.Y. and G.-W.M.; data curation, G.-S.Y. and G.-W.M.; writing—original draft preparation, G.-S.Y. and K.-H.K.; writing—review and editing, K.-H.K.; visualization, G.-S.Y. and G.-W.M.; supervision, K.-H.K. All authors have read and agreed to the published version of the manuscript.

Funding: This research was supported by the FRIEND (Fine Particle Research Initiative in East Asia Considering National Differences) Project through the National Research Foundation of Korea (NRF), funded by the Ministry of Science and ICT (NRF-2023M3G1A1090663), and also supported by Particulate Matter Management Specialized Graduate Program through the Korea Environmental Industry & Technology Institute (KEITI), funded by the Ministry of Environment (MOE).

Institutional Review Board Statement: Not applicable.

Informed Consent Statement: Not applicable.

Data Availability Statement: The data presented in this study are available on request from the corresponding author.

Conflicts of Interest: The authors declare no conflicts of interest.

References

1. National Air Emission Inventory and Research Center (NAIR). *2021 National Air Pollutant Emissions Inventory*; NAIR: Osong, Republic of Korea, 2023. Available online: <https://www.air.go.kr> (accessed on 20 July 2024).
2. Hsu, W.-T.; Chen, J.-L.; Lung, S.-C.C.; Chen, Y.-C. PM_{2.5} exposure of various microenvironments in a community: Characteristics and applications. *Environ. Pollut.* **2020**, *263*, 114522. [[CrossRef](#)] [[PubMed](#)]
3. Park, J.-M.; Han, Y.-J.; Cho, S.-H.; Kim, H.-W. Characteristics of carbonaceous PM_{2.5} in a small residential city in Korea. *Atmosphere* **2018**, *9*, 490. [[CrossRef](#)]
4. Wang, L.; Xiang, Z.; Stevanovic, S.; Ristovski, Z.; Salimi, F.; Gao, J.; Wang, H.; Li, L. Role of Chinese cooking emissions on ambient air quality and human health. *Sci. Total Environ.* **2017**, *589*, 173–181. [[CrossRef](#)]
5. Park, S.-K.; Choi, S.-J.; Kim, J.-Y.; Lee, H.-J.; Jang, Y.-K.; Bong, C.-K.; Kim, J.-H.; Hwang, U.-H. A study on the development of particulate matters emission factors from biomass burning: Mainly commercial meat cooking. *J. Korean Soc. Atmos. Environ.* **2011**, *27*, 426–435. (In Korean with English Abstract) [[CrossRef](#)]
6. Bandowe, B.A.M.; Lui, K.H.; Jones, T.; Bérubé, K.; Adams, R.; Niu, X.; Wei, C.; Cao, J.-J.; Lee, S.C.; Chuang, H.-C.; et al. The chemical composition and toxicological effects of fine particulate matter (PM_{2.5}) emitted from different cooking styles. *Environ. Pollut.* **2021**, *288*, 117754. [[CrossRef](#)]
7. Torkmahalleh, M.A.; Gorjinezhad, S.; Unluevcek, H.S.; Hopke, P.K. Review of factors impacting emission/concentration of cooking generated particulate matter. *Sci. Total Environ.* **2017**, *586*, 1046–1056. [[CrossRef](#)]
8. Jeong, H.; Park, D. Contribution of time-activity pattern and microenvironment to black carbon (BC) inhalation exposure and potential internal dose among elementary school children. *Atmos. Environ.* **2017**, *164*, 270–279. [[CrossRef](#)]
9. Seo, Y.-H.; Ku, M.-S.; Choi, J.-W.; Kim, K.-M.; Kim, S.-M.; Sul, K.-H.; Jo, H.-J.; Kim, K.-J.; Kim, K.-H. Characteristics of PM_{2.5} emission and distribution in a highly commercialized area in Seoul, Korea. *J. Korean Soc. Atmos. Environ.* **2015**, *31*, 97–104. (In Korean with English Abstract) [[CrossRef](#)]
10. Westerdahl, D.; Fruin, S.; Sax, T.; Fine, P.M.; Sioutas, C. Mobile platform measurements of ultrafine particles and associated pollutant concentrations on freeways and residential streets in Los Angeles. *Atmos. Environ.* **2005**, *39*, 3597–3610. [[CrossRef](#)]
11. Hagler, G.S.W.; Thoma, E.D.; Baldauf, R.W. High-resolution mobile monitoring of carbon monoxide and ultrafine particle concentrations in a near-road environment. *J. Air Waste Manag. Assoc.* **2010**, *60*, 328–336. [[CrossRef](#)] [[PubMed](#)]

12. Rakowska, A.; Wong, K.C.; Townsend, T.; Chan, K.L.; Westerdahl, D.; Ng, S.; Mocnik, G.; Drinovec, L.; Ning, Z. Impact of traffic volume and composition on the air quality and pedestrian exposure in urban street canyon. *Atmos. Environ.* **2014**, *98*, 260–270. [[CrossRef](#)]
13. Kim, K.H.; Woo, D.; Lee, S.-B.; Bae, G.-N. On-road measurements of ultrafine particles and associated air pollutants in a densely populated area of Seoul, Korea. *Aerosol Air Qual. Res.* **2015**, *15*, 142–153. [[CrossRef](#)]
14. Van den Bossche, J.; Peters, J.; Verwaeren, J.; Botteldooren, D.; Theunis, J.; De Baets, B. Mobile monitoring for mapping spatial variation in urban air quality: Development and validation of a methodology based on an extensive dataset. *Atmos. Environ.* **2015**, *105*, 148–161. [[CrossRef](#)]
15. Wang, S.; Ma, Y.; Wang, Z.; Wang, L.; Chi, X.; Ding, A.; Yao, M.; Li, Y.; Li, Q.; Wu, M.; et al. Mobile monitoring of urban air quality at high spatial resolution by low-cost sensors: Impacts of COVID-19 pandemic lockdown. *Atmos. Chem. Phys.* **2021**, *21*, 7199–7215. [[CrossRef](#)]
16. Kim, K.H.; Kwak, K.-H.; Lee, J.Y.; Woo, S.H.; Kim, J.B.; Lee, S.-B.; Ryu, S.H.; Kim, C.H.; Bae, G.-N.; Oh, I. Spatial mapping of a highly non-uniform distribution of particle-bound PAH in a densely populated urban area. *Atmosphere* **2020**, *11*, 496. [[CrossRef](#)]
17. Elen, B.; Peters, J.; Van Poppel, M.; Bleux, N.; Theunis, J.; Reggente, M.; Standaert, A. The aeroflux: A bicycle for mobile air quality measurements. *Sensors* **2013**, *13*, 221–240. [[CrossRef](#)] [[PubMed](#)]
18. MacNaughton, P.; Melly, S.; Vallarino, J.; Adamkiewicz, A.; Spengler, J.D. Impact of bicycle route type on exposure to traffic-related air pollution. *Sci. Total Environ.* **2014**, *490*, 37–43. [[CrossRef](#)] [[PubMed](#)]
19. Hankey, S.; Marshall, J.D. On-bicycle exposure to particulate air pollution: Particle number, black carbon, PM_{2.5}, and particle size. *Atmos. Environ.* **2015**, *122*, 65–73. [[CrossRef](#)]
20. Bertero, C.; Léon, J.-F.; Trédan, G.; Roy, M.; Argengaud, A. Urban-scale NO₂ prediction with sensors aboard bicycles: A comparison of statistical methods using synthetic observations. *Atmosphere* **2020**, *11*, 1014. [[CrossRef](#)]
21. Pattinson, W.; Longley, I.; Kingham, S. Using mobile monitoring to visualise diurnal variation of traffic pollutants across two near-highway neighbourhoods. *Atmos. Environ.* **2014**, *94*, 782–792. [[CrossRef](#)]
22. Samad, A.; Vogt, U. Investigation of urban air quality by performing mobile measurements using a bicycle (MOBAIR). *Urban Clim.* **2020**, *33*, 100650. [[CrossRef](#)]
23. Samad, A.; Vogt, U. Mobile air quality measurements using bicycle to obtain spatial distribution and high temporal resolution in and around the city center of Stuttgart. *Atmos. Environ.* **2021**, *244*, 117915. [[CrossRef](#)]
24. Robinson, E.S.; Gu, P.; Ye, Q.; Li, H.Z.; Shah, R.U.; Apte, J.S.; Robinson, A.L.; Presto, A.A. Restaurant impacts on outdoor air quality: Elevated organic aerosol mass from restaurant cooking with neighborhood-scale plume extents. *Environ. Sci. Technol.* **2018**, *52*, 9285–9294. [[CrossRef](#)] [[PubMed](#)]
25. Choi, S.-Y.; Park, S.-W.; Byun, J.-Y.; Han, Y.-J. Characteristics of locally occurring high PM_{2.5} concentration episodes in a small city in South Korea. *Atmosphere* **2021**, *12*, 86. [[CrossRef](#)]
26. Park, S.-W.; Choi, S.-Y.; Byun, J.-Y.; Kim, H.; Kim, W.-J.; Kim, P.-R.; Han, Y.-J. Different characteristics of PM_{2.5} measured in downtown and suburban areas of a medium-sized city in South Korea. *Atmosphere* **2021**, *12*, 832. [[CrossRef](#)]
27. Cao, C.; Yang, Y.; Lu, Y.; Schultze, N.; Gu, P.; Zhou, Q.; Xu, J.; Lee, X. Performance evaluation of a smart mobile air temperature and humidity sensor for characterizing intracity thermal environment. *J. Atmos. Ocean. Technol.* **2020**, *37*, 1891–1905. [[CrossRef](#)]
28. Li, B.; Cao, R.; Wang, Z.; Song, R.-F.; Peng, Z.-R.; Xiu, G.; Fu, Q. Use of multi-rotor unmanned aerial vehicles for fine-grained roadside air pollution monitoring. *J. Trans. Res. Board* **2019**, *2673*, 169–180. [[CrossRef](#)]
29. Liu, X.; Hadiatullah, H.; Zhang, X.; Hill, L.D.; White, A.H.A.; Schnelle-Kreis, J.; Bendl, J.; Jakobi, G.; Schlöter-Hai, B.; Zimmermann, R. Analysis of mobile monitoring data from the microAeth[®] MA200 for measuring changes in black carbon on the roadside in Augsburg. *Atmos. Meas. Tech.* **2021**, *14*, 5139–5151. [[CrossRef](#)]
30. Alas, H.D.C.; Müller, T.; Weinhold, K.; Pfeifer, S.; Glojek, K.; Gregoric, A.; Mocnik, G.; Drinovec, L.; Costabile, F.; Ristorini, M.; et al. Performance of micro aethalometers: Real-world field intercomparisons from multiple mobile measurement campaigns in different atmospheric environments. *Aero. Air Qual. Res.* **2020**, *20*, 2640–2653. [[CrossRef](#)]
31. Park, Y.; Park, H.-S.; Han, S.; Hwang, K.; Lee, S.; Choi, J.-Y.; Lee, J.-B.; Lee, S.-H.; Kwak, K.-H.; Kim, J.-J.; et al. Intra-community scale variability of air quality in the center of a megacity in South Korea: A high-density cost-effective sensor network. *Appl. Sci.* **2021**, *11*, 9105. [[CrossRef](#)]
32. Lung, S.-C.C.; Wang, W.-C.V.; Wen, T.-Y.J.; Liu, C.-H.; Hu, S.-C. A versatile low-cost sensing device for assessing PM_{2.5} spatiotemporal variation and quantifying source contribution. *Sci. Total Environ.* **2020**, *716*, 137145. [[CrossRef](#)]
33. Apte, J.S.; Messier, K.P.; Gani, S.; Brauer, M.; Kirchstetter, T.W.; Lunden, M.M.; Marshall, J.D.; Portier, C.J.; Vermeulen, R.C.H.; Hamburg, S.P. High-resolution air pollution mapping with Google street view cars: Exploiting big data. *Environ. Sci. Technol.* **2017**, *51*, 6999–7008. [[CrossRef](#)]
34. Messier, K.P.; Chambliss, S.E.; Gani, S.; Alvarez, R.; Brauer, M.; Choi, J.J.; Hamburg, S.P.; Kerckhoffs, J.; LaFranchi, B.; Lunden, M.M.; et al. Mapping air pollution with Google street view cars: Efficient approaches with mobile monitoring and land use regression. *Environ. Sci. Technol.* **2018**, *52*, 12563–12572. [[CrossRef](#)] [[PubMed](#)]
35. Lee, S.-H.; Kwak, K.-H. Assessing 3-D spatial extent of near-road air pollution around a signalized intersection using drone monitoring and WRF-CFD modeling. *Int. J. Environ. Res. Public Health* **2020**, *17*, 6915. [[CrossRef](#)]
36. Park, S.-W.; Han, Y.-J.; Hong, J.-H.; Lee, T.-H. PM_{2.5}-bound inorganic and nonpolar organic compounds in Chuncheon, Korea. *Asian J. Atmos. Environ.* **2022**, *16*, 2022111. [[CrossRef](#)]

37. Kim, S.-C.; Lee, T.-J.; Jeon, J.-M.; Kim, D.-S.; Jo, Y.-M. Emission characteristics and control device effectiveness of particulate matters and particulate-phase PAHs from urban charbroiling restaurants: A field test. *Aero. Air Qual. Res.* **2020**, *20*, 2185–2195. [[CrossRef](#)]
38. Yao, D.; Lyu, X.; Lu, H.; Zeng, L.; Liu, T.; Chan, C.K.; Guo, H. Characteristics, sources and evolution processes of atmospheric organic aerosols at a roadside site in Hong Kong. *Atmos. Environ.* **2021**, *252*, 118298. [[CrossRef](#)]
39. Park, S.K.; Kim, D.K.; Hwang, U.H.; Lee, J.J.; Lee, J.B.; Bae, I.S.; Eo, S.-M.; Jung, K. Emission characteristics of air pollutants from meat charbroiling. *J. Clim. Change Res.* **2015**, *6*, 311–318, (In Korean with English Abstract). [[CrossRef](#)]
40. Sim, S.; Jeong, S.; Park, H.; Park, C.; Kwak, K.-H.; Lee, S.-B.; Kim, C.H.; Lee, S.; Chang, J.; Kang, H.; et al. Co-benefit potential of urban CO₂ and air quality monitoring: A study on the first mobile campaign and building monitoring experiments in Seoul during the winter. *Atmos. Pollut. Res.* **2020**, *11*, 1963–1970. [[CrossRef](#)]
41. Kwak, K.-H.; Han, B.-S.; Park, K.; Moon, S.; Jin, H.-G.; Park, S.-B.; Baik, J.-J. Inter- and intra-city comparisons of PM_{2.5} concentration changes under COVID-19 social distancing in seven major cities of South Korea. *Air Qual. Atmos. Health* **2021**, *14*, 1155–1168. [[CrossRef](#)]
42. Hwang, K.; Kim, J.; Lee, J.Y.; Park, J.-S.; Park, S.; Lee, G.; Kim, C.H.; Kim, P.; Shin, S.H.; Lee, K.Y.; et al. Physicochemical characteristics and seasonal variations of PM_{2.5} in urban, industrial, and suburban areas in South Korea. *Asian J. Atmos. Environ.* **2023**, *17*, 19. [[CrossRef](#)]

Disclaimer/Publisher’s Note: The statements, opinions and data contained in all publications are solely those of the individual author(s) and contributor(s) and not of MDPI and/or the editor(s). MDPI and/or the editor(s) disclaim responsibility for any injury to people or property resulting from any ideas, methods, instructions or products referred to in the content.